Advances in Science and Technology *Online: 2010-10-27*
ISSN: 1662-0356, Vol. 62, pp 131-140
doi:10.4028/www.scientific.net/AST.62.131

Theoretical and Experimental Analyses of Colloidal Processing of Nanoparticles

Yoshihiro Hirata[1,a], Koichiro Matsushima[1,b], Shinichi Baba[1,c], Naoki Matsunaga[1,d] and Soichiro Sameshima[1,e]

Department of Chemistry, Biotechnology and Chemical Engineering,
Kagoshima University, 1-21-40 Korimoto, Kagoshima 890-0065, Japan

[a]hirata@apc.kagoshima-u.ac.jp, [b]k-matsushima@apc.kagoshima-u.ac.jp,
[c]s-baba@apc.kagoshima-u.ac.jp, [d]n-matsunaga@apc.kagoshima-u.ac.jp,
[e]samesima@apc.kagoshima-u.ac.jp

Keywords: Colloidal particles, Dispersion, Flocculation, Colloidal phase diagram, Pressure filtration, Phase transition.

Abstract. The stability of dispersed and flocculated colloidal particles under 1 atm and applied pressure was discussed thermodynamically with the activity and chemical potential defined by Henry's law and Raoult's law. The calculated result under 1 atm is represented by a colloidal phase diagram as functions of surface potential and solid content of particles. Application of pressure accelerates the phase transition from dispersed to flocculated suspension. The phase transition pressure, which is observed in the applied pressure-suspension height relation during pressure filtration at a constant crosshead speed of piston, is affected by (1) particle concentration, (2) particle size, (3) surface potential, (4) degree of dissociation of polyelectrolyte dispersant and (5) applied electric field (DC and AC). The influence of above factors was discussed theoretically and experimentally.

Introduction

Colloidal processing is widely applied to improve microstructures and properties of advanced ceramics. The basic concept of interaction between colloidal particles is given by the DLVO theory. Especially, electrostatic stabilization, steric stabilization and electrosteric stabilization are key technologies to disperse nanometer- or submicrometer-sized particles in an aqueous solution. The above technologies are usually discussed under atmospheric pressure. However, a pressure is applied to the stabilized colloidal particles to consolidate by filtration using gypsum mold (suction pressure), pressure filtration or doctor blade. The stability of colloidal particles under an applied pressure is a key factor to understand the green structure formed. However, little analysis has been reported for the influence of applied pressure on the colloidal stability.

In our previous paper [1], we established the thermodynamics of a colloidal suspension containing dispersed and flocculated particles at 1 atm. The maximum interaction energy between electrostatically-stabilized colloidal particles by DLVO theory is related to the enthalpy for migration of dispersed particles to form flocculated particles. From the derived thermodynamic relations, we constructed a one-component colloidal phase diagram as functions of surface potential and volume fraction of charged particles, as shown in Fig. 1. The liquidus line corresponds to packing density of colloidal particles, which increases as surface potential increases. Flocculated particles are formed below a critical surface potential (solidus line). When a particle size decreases, the surface potential for solidus line increases and the packing density decreases. The above concepts agreed with the experimentally measured packing behavior of colloidal particles in a size range from 10 to 1000 nm.

In addition, it was clarified that the dispersed colloidal particles transform into flocculated particles at a critical applied pressure. In our previous papers [2,3], new filtration theories of flocculated particles at a constant crosshead speed of piston or at a constant applied pressure were

proposed. Experimentally measured results were well explained by the proposed theories. The important factors affecting the phase transition pressure (ΔP_{tc}) were identified to be zeta potential, solid concentration of suspension, size of particles, polyelectrolyte dispersant and direct and alternating current electric fields [4]. In this paper, the influence of the above factors on ΔP_{tc} is theoretically discussed and experimentally analyzed.

Activity and Chemical Potential of Dispersed and Flocculated Particles at 1 atm

Figure 2 shows a structure model of colloidal suspension (1 l volume) containing both dispersed and flocculated particles. The suspension contains n_i spherical particles of radius r. The total volume of n_i particles is $C_0 = n_i v$ ($v = 4\pi r^3/3$, volume of one particle). The dispersed particles in a suspension collide to form flocculated particles and both the sates behave as atoms in a solid solution. The collision rate is usually expressed by a second order reaction (Eq.(1)),

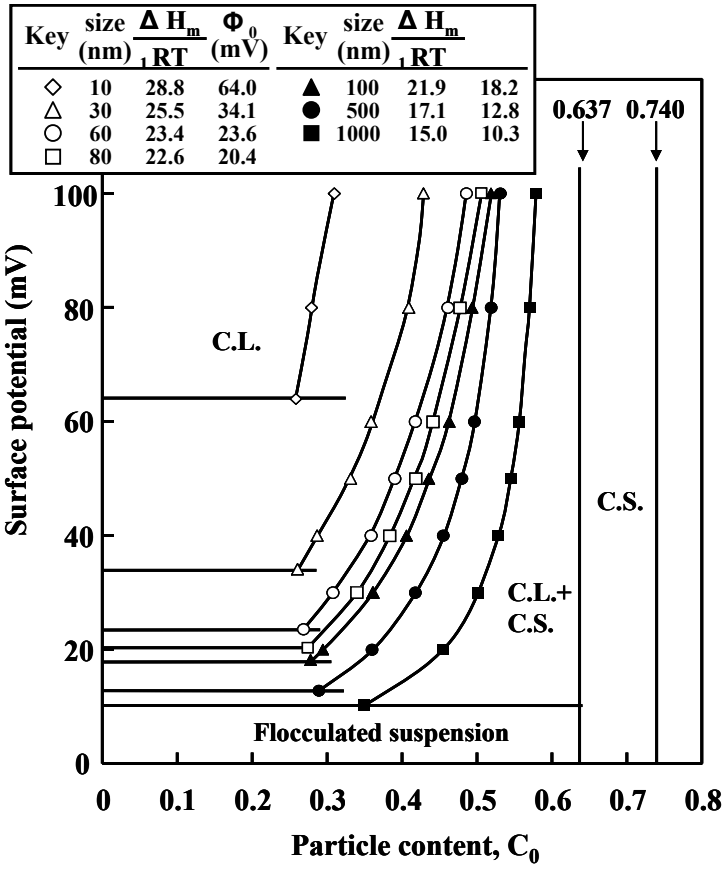

Fig. 1. Colloidal phase diagrams for particle size range from 10 to 1000 nm. C.L. : colloidal liquid, C.S. : colloidal solid.

$$-\frac{dN_d}{dt} = kN_d^2 \qquad (1)$$

where k is the rate constant and N_d the concentration of dispersed particles (mol/l). This equation is easily solved under the conditions of $N_d = n_i / n_A$ at t = 0 and $N_d = n_d / n_A$ at t = t, where n_d is the number of dispersed particles ($n_d = n_i\alpha$) and α the molar fraction (volume fraction) of dispersed particles to the total particle content, and n_A the Avogadro number. The integrated form is given by Eq.(2),

$$\frac{1}{n_d} - \frac{1}{n_i} = \frac{1}{n_i\alpha} - \frac{1}{n_i} = \left(\frac{k}{n_A}\right)t \qquad (2)$$

From Eq.(2), α is expressed by Eq. (3),

$$\alpha = \frac{1}{1 + n_i k_1 t} \qquad (3)$$

where k_1 is equal to k / n_A. That is, the fraction of dispersed particles is a function of settling time and decreases at a longer time. The activity of dispersed

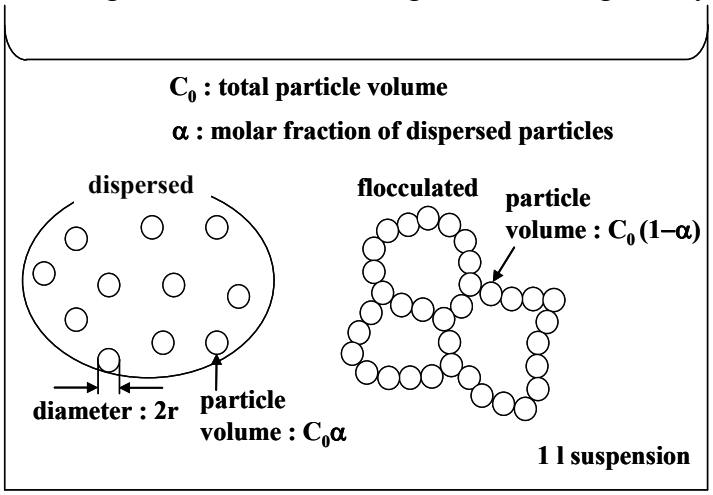

Fig. 2. A suspension model containing dispersed and flocculated particles.

particles (a_d) is expressed by Henry's law as like as atoms in a solid solution and equal to the product of the molar fraction (α) of dispersed particles and the activity coefficient (γ^0) expressed by C_0 / C_{max} (C_0 : total volume fraction of dispersed and flocculated particles, C_{max} : maximum packing density of particles). For the close packing and random close packing models, C_{max} is 0.740 and 0.637, respectively. The γ^0 value results in 1 for $C_0 = C_{max}$. That is, the activity and chemical potential of dispersed particles are given by Eqs.(4) and (5), respectively.

$$a_d = \gamma^0\alpha = \gamma^0\left(\frac{1}{1+n_i k_1 t}\right) = \left(\frac{C_0}{C_{max}}\right)\left[\frac{1}{1+\left(\frac{C_0}{v}\right)k_1 t}\right] \tag{4}$$

$$\mu_d = \mu_{d0} + RT\ln(\gamma^0\alpha) = \mu_{d0} + RT\ln\left(\frac{1}{C_{max}}\right) + RT\ln\left[\frac{1}{\left(\frac{1}{C_0}\right)+\left(\frac{k_1}{v}\right)t}\right] \tag{5}$$

The μ_{d0} value represents the chemical potential of dispersed particles for $\alpha = 1$ and $\gamma^0 = 1$. The activity of flocculated particles (a_g) follows Raoult's law and is expressed as $(1-\alpha)$ using the Gibbs-Duhem equation. Equations (6) and (7) represent the activity and chemical potential of flocculated particles, respectively.

$$a_g = 1-\alpha = \frac{n_i k_1 t}{1+n_i k_1 t} = \frac{1}{1+\frac{1}{\left(\frac{C_0}{v}\right)k_1 t}} \tag{6}$$

$$\mu_g = \mu_{g0} + RT\ln(1-\alpha) = \mu_{g0} + RT\ln\left[\frac{1}{1+\frac{1}{\left(\frac{C_0}{v}\right)k_1 t}}\right] \tag{7}$$

The μ_{g0} corresponds to the chemical potential of flocculated particles at $\alpha = 0$.

Figure 3 shows the schematic relation of a and μ as a function of time. The a_d decreases from γ^0 at $t = 0$ to 0 at $t = \infty$. On the other hand, the a_g increases from 0 at $t = 0$ to 1 at $t = \infty$. This change is accompanied by the change in μ_g from $-\infty$ at $t = 0$ to μ_{g0} at $t = \infty$. The important note is that the collision of dispersed particles stops at a critical time t_{c1} for $\Delta\mu = 0$, because the equilibrium state is achieved. The time t_{c1} required to reach the equilibrium state is determined from Eqs.(5) and (7),

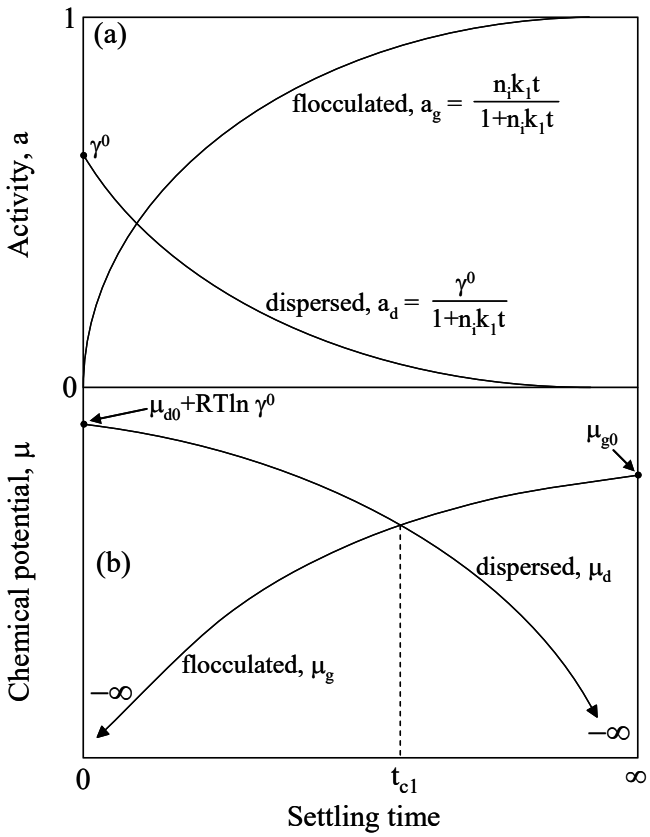

Fig. 3. Schematic relation of activity (a) and chemical potential (b) of dispersed and flocculated particles as a function of settling time.

$$t_{c1} = \frac{\gamma^0}{\left(\frac{C_0}{v}\right)k_1} \exp\left(-\frac{\Delta\mu_0}{RT}\right) \tag{8}$$

where $\Delta\mu_0$ represents $\mu_{g0}-\mu_{d0}$. The above analysis is applied to discuss the influence of pressure on μ_d and μ_g in section 4. Before section 4, we show the experimental results of effect of pressure on the consolidation of nanoparticles.

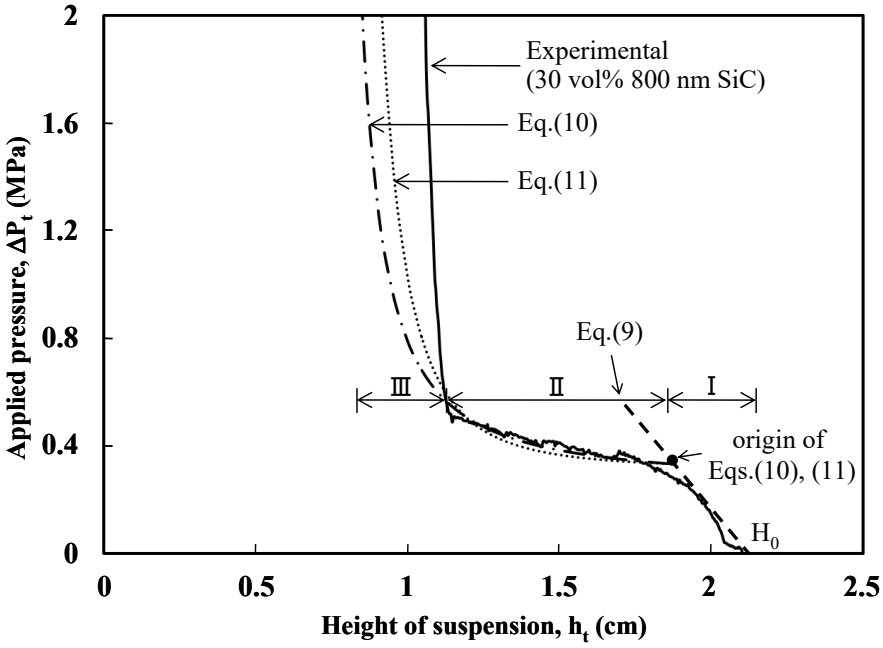

Fig. 4. Comparison of applied pressure-suspension height relation between experiment and proposed theories (Eqs. 9, 10 and 11) for the pressure filtration process of 30 vol% SiC suspension at pH 7.0.

Phase Transition of Colloidal Suspensions

A phase transition from a dispersed suspension to a flocculated suspension occurs at a critical applied pressure (ΔP_{tc}) for nanoparticles of 20–800 nm size [2]. Figure 4 shows the typical relation between applied pressure (ΔP_t) of filtration and height (h_t) of 30 vol% SiC suspension at 0.2 mm/min of crosshead speed of piston. The isoelectric point of the SiC particles was pH 2.8. A low viscosity suspension was prepared with negatively charged SiC particles at pH 7. In the early region I of filtration, the applied pressure increased linearly with the difference of H_0-h_t (H_0: initial height of suspension). This result is explained by the established filtration theory for dispersed particles by Eq. (9),

$$\Delta P_t = \left(\frac{\eta\alpha_c v_0}{n}\right)(H_0 - h_t) \tag{9}$$

where η is the viscosity of filtration, α_c the specific resistance of porous consolidated layer, v_0 the crosshead speed of piston, and n the system parameter ($= (1-C_0-\varepsilon_c)/\varepsilon_c$, ε_c the volume fraction of voids in the consolidated layer). However, an almost plateau region of ΔP_t appeared in region II. This change in the consolidation behavior is related to the phase transition from a dispersed suspension

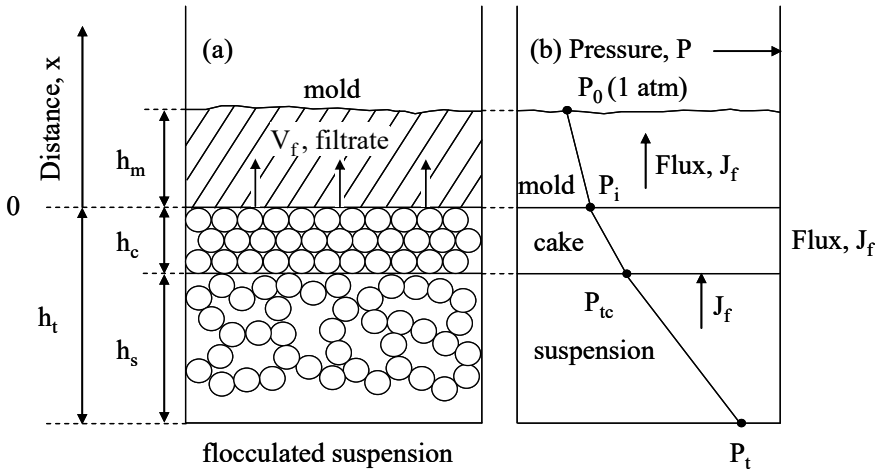

Fig. 5. Schematic structure of colloidal system (a) after the phase transition from dispersed to flocculated suspension and hydraulic pressure profile of the filtration

to a flocculated suspension at a critical applied pressure. As a result, the consolidation behavior of the flocculated particles deviated from the filtration theory for well dispersed particles.

Figure 5 shows the schematic structure of the suspension and the hydraulic pressure profile across the mold, consolidated layer and flocculated suspension. In our previous papers [1,2], we developed new filtration theories for a flocculated suspension. The relation between suspension height and filtration pressure, ΔP_s (= P_t–P_i), for an initially flocculated suspension is calculated by Eqs. (10) or (11),

$$\Delta P_t = \eta v_0 B S^2 (H_0 C_0)^2 \int_{H_0}^{h_s} \frac{h_s}{(h_s - H_0 C_0)^3} dh_s$$
$$= \eta v_0 B S^2 (H_0 C_0)^2 \frac{1}{2}\left\{ \frac{H_0}{H_0^2 (1-C_0)^2} - \frac{h_s}{(h_s - H_0 C_0)^2} + \frac{1}{H_0 (1-C_0)} - \frac{1}{(h_s - H_0 C_0)} \right\} \quad (10)$$

$$\Delta P_t = \eta v_0 \left(\frac{36B}{D^2} \right) (H_0 C_0)^4 \int_{H_0}^{h_s} \frac{1}{h_s (h_s - H_0 C_0)^3} dh_s$$
$$= \eta v_0 \left(\frac{36B}{D^2} \right) (H_0 C_0)^4 \left\{ -\frac{1}{2H_0 C_0} \left[\frac{1}{(h_s - H_0 C_0)^2} - \frac{1}{(H_0 - H_0 C_0)^2} \right] \right.$$
$$\left. + \frac{1}{(H_0 C_0)^2} \left[\frac{1}{(h_s - H_0 C_0)} - \frac{1}{(H_0 - H_0 C_0)} \right] + \frac{1}{(H_0 C_0)^3} \left[\ln\left(\frac{h_s - H_0 C_0}{H_0 - H_0 C_0} \right) - \ln\left(\frac{h_s}{H_0} \right) \right] \right\} \quad (11)$$

B, S and D in Eqs.(10) and (11) are the ratio of shape factor to the tortuosity constant, the ratio of the total solid surface area to the apparent volume and particles diameter, respectively. In Eq.(10), BS^2 value is treated as a constant value. In Eq.(11), S value is treated as a function of suspension height (h_s) by Eq.(12).

$$S = \frac{6(1-\varepsilon_s)}{D} = \left(\frac{6 C_0 H_0}{D} \right) \frac{1}{h_s} \quad (12)$$

The ε_s in Eq.(12) indicates the volume fraction of solution in the flocculated suspension. Substitution of Eq.(12) for Eq.(10) before the integration provides Eq.(11). As seen in Fig.4, the experimental result was well fitted by Eqs.(10) and (11). In the final region III, Eq.(11) gives a better agreement than Eq.(10) for the measured result. The factors affecting ΔP_{tc} are the zeta potential, concentration of suspension, size of particles, polyelectrolyte dispersant and electric field.

Figure 6 shows ΔP_{tc} of several nanometer-sized particles as a function of the zeta potential [2]. Increase of zeta potential and increase of particle size shift ΔP_{tc}

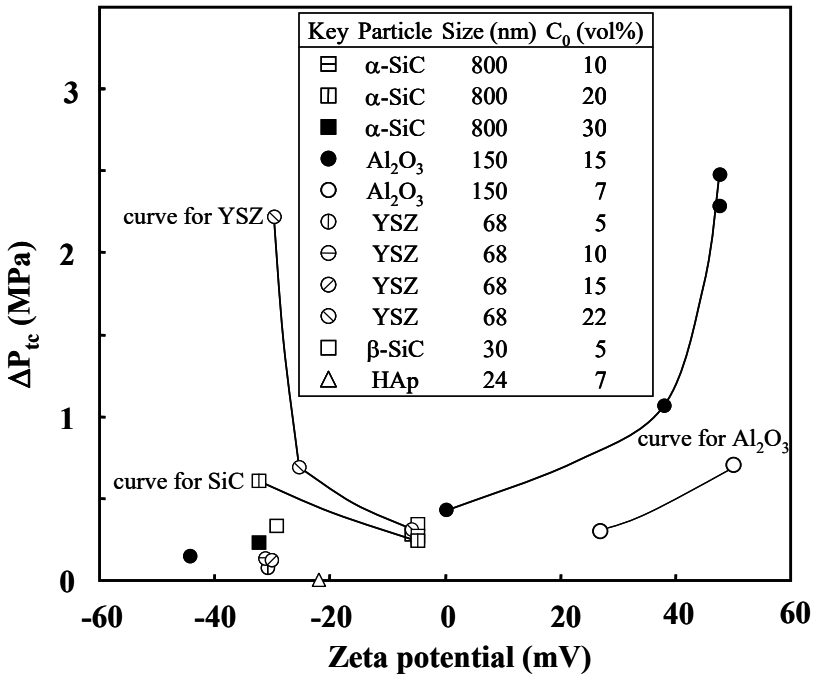

Fig. 6. Phase transition pressure and zeta potential for several nanometer-sized particles. YSZ and HAp represent yttria-stabilized zirconia and hydroxyapatite respectively.

to a high pressure. The ΔP_{tc} is also influenced by particle concentration, dissociation and amount of polyelectrolyte added. The addition of a large amount of highly charged polyacrylic ammonium suppressed the phase transition from dispersed to flocculated state of colloidal particles at a given applied pressure [4,5]. When an alternating electric field was applied, the ΔP_{tc} value decreased drastically.

Factors affecting colloidal phase transition

The chemical potential of dispersed (μ_d) and flocculated (μ_g) particles is related to pressure and temperature by Eqs.(13) and (14), respectively.

$$d\mu_d = \overline{V_d}dP - \overline{S_d}dT \quad (13)$$

$$d\mu_g = \overline{V_g}dP - \overline{S_g}dT \quad (14)$$

$\overline{V}$ and $\overline{S}$ are the partial molar volume and partial molar entropy of particles in a suspension, respectively. Integration of Eqs.(13) and (14) at a constant temperature yields Eqs.(15) and (16), respectively, under the constant $\overline{V}$ value.

$$\mu_d(P) - \mu_d(P=1) = \overline{V_d}(P-1) \quad (15)$$

$$\mu_g(P) - \mu_g(P=1) = \overline{V_g}(P-1) \quad (16)$$

The μ (P = 1) value in Eqs.(15) and (16) indicates the chemical potential of particles at 1 atm. The phase transition pressure ($\Delta P_{tc} = P_t - 1$ atm) is solved under the condition of $\mu_d(P) = \mu_g(P)$ for Eqs.(15) and (16).

$$\Delta P_{tc} = \frac{\mu_d(P=1) - \mu_g(P=1)}{\overline{V_g} - \overline{V_d}} \quad (17)$$

The phase transition pressure is closely related to the difference of chemical potential between dispersed and flocculated particles at 1 atm. The μ (P = 1) value is controlled by C_0 (initial concentration), v (volume of one particles) and k_1 (rate constant of flocculation) as a presented by Eqs.(5) and (7), and discussed in a latter part. On the other hand, $\overline{V_g}$ for flocculated particles of Avogadro number is larger than $\overline{V_d}$ for well dispersed particles because flocculated particles of 1 mol occupy a large space in the suspension than dispersed particles of 1 mol that can be densely

Table 1 Summary of the influence of concentration of particles (C_0), volume of one particle (v) and rate constant (k) for flocculation on phase transition pressure (ΔP_{tc}).

Factor	Influence	Chemical potential		Phase transition pressure	
		μ_d dispersed	μ_g flocculated	ΔP_{tc}	
C_0 (concentration)	increase	↑	↑	↓ (B-1)*	↑ (B-2)*
	decrease	↓	↓	↑ (B-1)	↓ (B-2)
v (size)	increase	↑	↓	↑	
	decrease	↓	↑	↓	
k (rate constant)	increase	↓	↑	↓	
	decrease	↑	↓	↑	

↑ : increased, ↓ : decreased, * : See Fig. 6

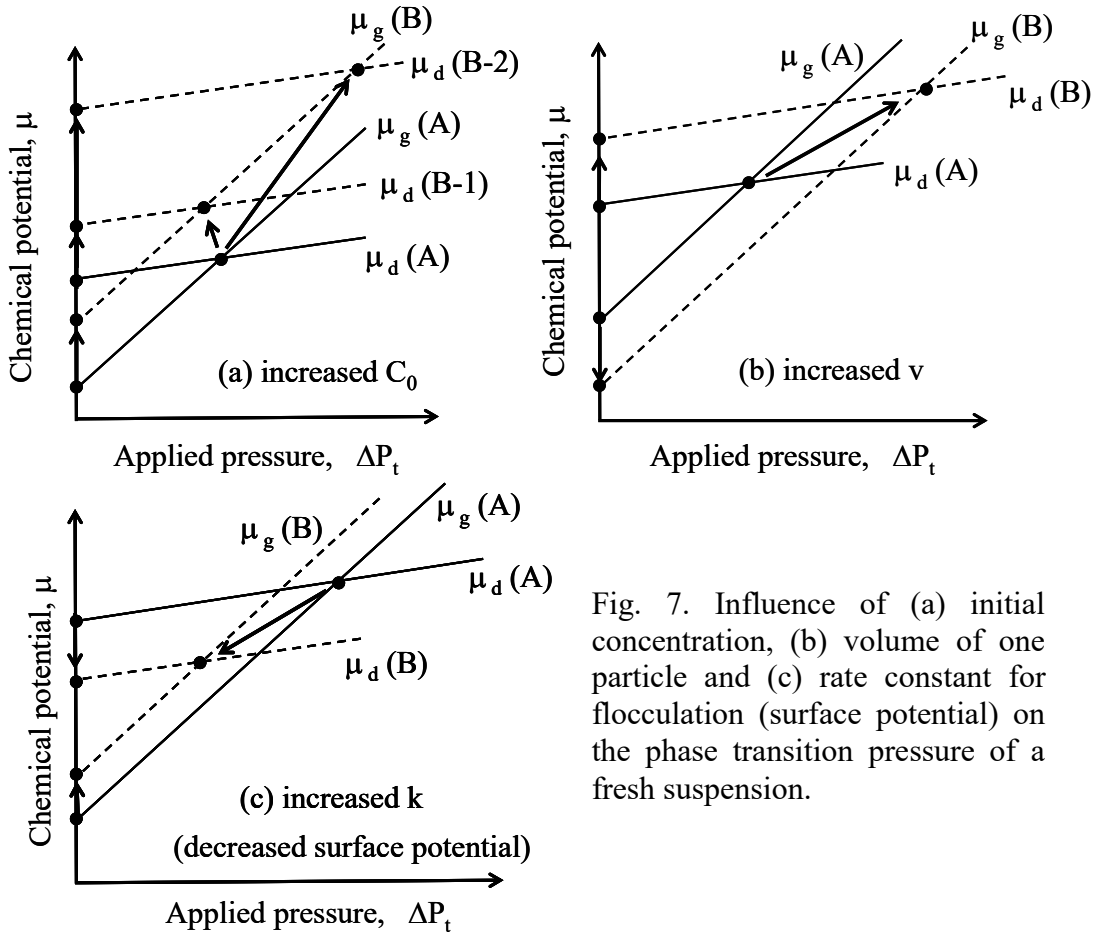

Fig. 7. Influence of (a) initial concentration, (b) volume of one particle and (c) rate constant for flocculation (surface potential) on the phase transition pressure of a fresh suspension.

packed.

Figure 7 shows the influence of (a) initial concentration, (b) volume of one particle and (c) rate constant for flocculation (surface potential) on the phase transition pressure of a fresh suspension ($t \ll t_{cl}$). The intercept of μ_d and μ_g lines indicates the chemical potential at 1 atm and the slope corresponds to $\overline{V}$. The increased C_0 causes the increase of $\mu_d(P = 1)$ and $\mu_g(P = 1)$ from Eqs.(5) and (7) at a given time. As a result, the ΔP_{tc} at the intersection of μ_d and μ_g lines may decrease or increase, depending on the degree of increase of μ of dispersed and flocculated particles. The size effect is also discussed with Eqs.(5) and (7). The increase in v leads to the increase of $\mu_d(P = 1)$ and the decrease of $\mu_g(P = 1)$. As a result, the ΔP_{tc} increases. The increase of k_1, which is associated with the decrease of surface potential, causes the decrease of $\mu_d(P = 1)$ and the increase of $\mu_g(P = 1)$, resulting in the decrease of ΔP_{tc}. The above effects are summarized in Table 1. The ΔP_{tc} increases in the following conditions: (1) increase of particle concentration (B–2 case in Fig. 7 (a)), (2) increase of particle size and (3) decrease of rate constant (increase of surface potential). The theoretically derived concept on ΔP_{tc} was in accordance with the experimentally measured tendency in Fig. 6.

Influence of Dispersant and Electric Field

Figure 8 shows the influence of polyacrylic ammonium (PAA, $(-CH_2-CHCOONH_4-)_n$, molecular weight 10000) on the phase transition of alumina particle suspensions of 7 vol% solid. At pH 3.0, the alumina particles without PAA were charged positively (isoelectric point pH 7.7) and dispersed well because of the strong electrostatic repulsion. The ΔP_{tc} to form a flocculated suspension was measured at 0.63 MPa. PAA added in the alumina suspension at pH 3.0, which exists as a form of neutral polymer, is adsorbed on the surfaces of positively charged alumina particles [6,7]. This adsorption of neutral PAA reduces the electrostatic repulsive interaction between charged alumina particles. The addition of excess PAA did not affect the shape of the P_t–V_f curve (Fig. 8 (b)) as compared with the curve of Fig. 8 (a). However, the filtration pressure

increased significantly. This result reflects that (1) a thick layer of neutral PAA is formed on the Al_2O_3 particles, (2) PAA–adsorbed Al_2O_3 particles are flocculated by the applied pressure during the filtration, and (3) the relatively high filtration pressure is related to the difficulty of elimination of the solution through thick PAA layers on the Al_2O_3 surface. That is, the increase of ΔP_{tc} with addition of neutral PAA is interpreted to be equivalent to the increased v in Table 1. On the other hand, the addition of a large amount of negatively charged PAA to an alumina suspension at pH 7.0 suppressed the colloidal phase change and maintained the dispersion state at a high applied pressure (> 3.5 MPa). This result is interpreted by the coupling of increased v and decreased k in Table 1. The above result indicates that steric or electrosteric stabilization effect of excess polyelectrolyte leads to the increased ΔP_{tc}.

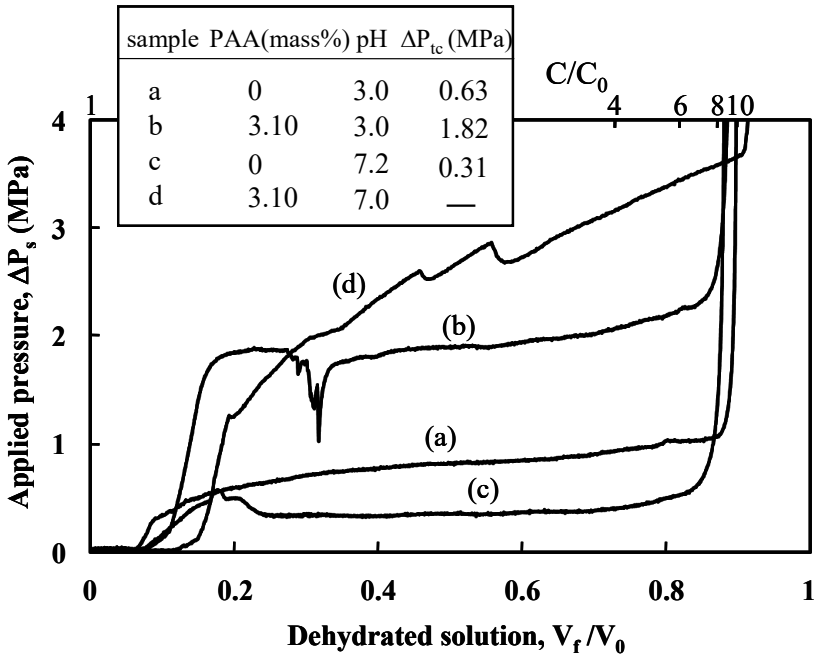

Fig. 8. Relation between normalized filtration volume (V_f / V_0) and applied pressure for alumina suspensions with and without PAA. V_0 : initial suspension volume.

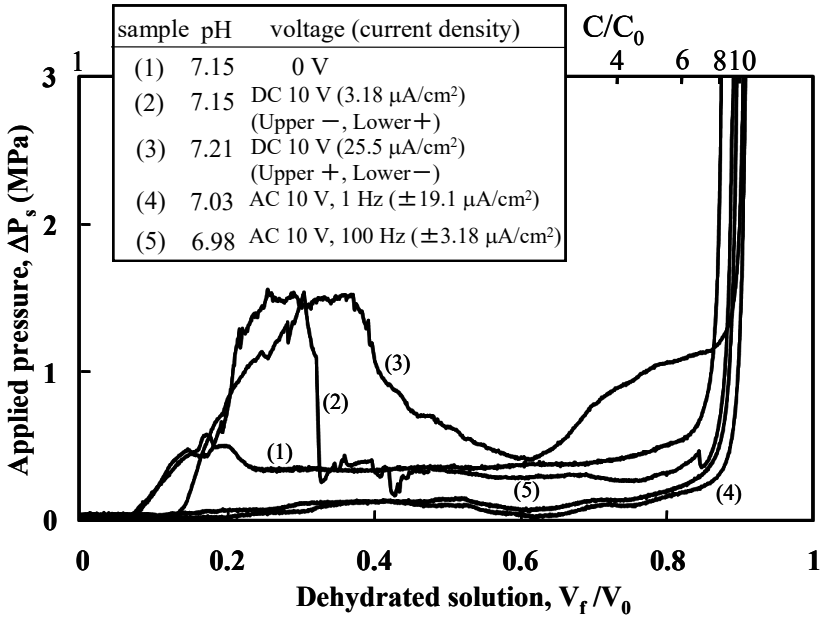

Fig. 9. Influence of electric field on the phase transition of 7 vol% alumina suspension at pH 7.0–7.2 during pressure filtration.

Figure 9 shows the effect of electric field on the phase transition of 7 vol% alumina suspension at pH 7.0–7.2 during the pressure filtration at 0.2 mm/min of crosshead speed of piston. Under a direct current field the applied pressure showed a maximum value as a function of volume of filtrate and then decreased to a nearly constant value. The application of alternating current field decreased drastically the filtration pressure, accelerating the phase transition to flocculated suspension. As shown in Fig. 10, application of direct current field causes the migration of ions in a solution and in diffuse layers to cathode and anode. The small ions move faster than large charged particles. This migration of free ions decreases the ionic concentration around charged particles and enhances the repulsive force between two charged particles. As a result, the dispersion of charged particles is enhanced and applied pressure increases linearly with increasing volume of filtrate. That is, DC effect is equivalent to the increased surface potential in Table 1 and increases ΔP_{tc} value. In contrast to DC field, AC field promotes the

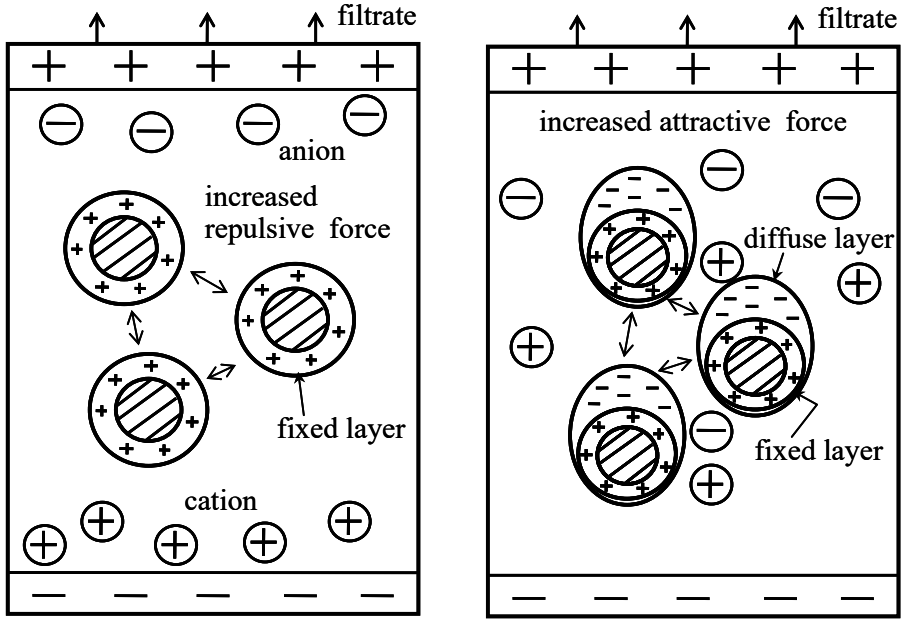

Fig. 10. Scheme explaining effects of (a) direct and (b) alternating current fields on the phase transition of colloidal suspensions.

flocculation of charged particles. The periodic polarization of ions in diffuse layers is enhanced by AC field. The polarization of positive and negative ions in the electric double layers produces the electrostatic attraction between polarized colloidal particles, leading to the formation of flocculated particles. This AC effect is equivalent to the decreased surface potential (increased k value) in Table 1. The above concept is supported by the calculation of migration distance of charged alumina particles and H^+, OH^- and Cl^- ions included in a compressed colloidal suspension, under an applied DC or AC field. This result will be reported soon in a next paper.

Conclusions

The stability of colloidal nanoparticles under applied pressure was theoretically and experimentally analyzed. A phase transition from a dispersed suspension to a flocculated suspension occurs at a critical applied pressure (ΔP_{tc}) for nanoparticles of 20−800 nm size. This phase transition can be measured in the applied pressure-suspension height relation during pressure filtration at a constant crosshead speed of piston. The consolidation behavior of a flocculated suspension was well fitted by proposed new filtration theories. The ΔP_{tc} value is closely related to the difference of chemical potential between dispersed and flocculated particles at 1 atm. The chemical potential of colloidal particles at 1 atm is controlled by concentration of particles, volume (size) of one particles and rate constant of flocculation (surface potential). The ΔP_{tc} increases in the following conditions: (1) increase of particle concentration for the condition that chemical potential of dispersed particles is greatly increased by the increased concentration, (2) increase of particles size, and (3) increase of surface potential. The steric or electrosteric stabilization of colloidal particles by excess polyelectrolyte leads to the increased ΔP_{tc}. Application of direct current field during pressure filtration provides a temporary increase of applied pressure as a function of the amount of filtrate. In contrast to DC field, AC field accelerates the flocculation of charged particles and leads to the decreased applied pressure during filtration.

References

[1] Y. Hirata and Y. Tanaka: J. Ceram. Process. Res., Vol. 9 (2008), pp. 362-371.

[2] Y. Hirata and Y. Tanaka: J. Am. Ceram. Soc., Vol. 91 (2008), pp. 819-824.

[3] Y. Tanaka, Y. Hirata, N. Matsunaga, S. Sameshima and T. Yoshidome: J. Ceram. Soc. Japan, Vol. 115 (2007), pp. 786-791.

[4] Y. Hirata, H. Uchima, Y. Tanaka and N. Matsunaga: J. Am. Ceram. Soc., Vol. 92 (2009), pp. 557-562.

[5] Y. Hirata, Y. Tanaka, S. Nakagawa and N. Matsunaga: J. Ceram. Process. Res., Vol. 10 (2009), pp. 311-318.

[6] Y. Hirata, J. Kamikakimoto, A. Nishimoto and Y. Ishihara: J. Ceram. Soc. Japan, Vol. 100 (1992), pp. 7-19.

[7] Y. Hirata, A. Nishimoto and Y. Ishihara: J. Ceram. Soc. Japan, Vol. 100 (1992), pp. 983-990.